# Fast Motion-free LiDAR System Based upon Ferroelectric Liquid Crystal Dammann Grating

**Zheng-Nan Yuan[1], Zhi-bo Sun[1], H. S. Kwok[1], A. K. Srivastava[1]**

Email:zyuanae@connect.ust.hk

[1]State Key Laboratory of Advanced Displays and Optoelectronics Technologies, Department of Electronic and Computer Engineering, Hong Kong University of Science and Technology, Clear Water Bay, Kowloon, Hong Kong

Key words: Ferroelectric liquid crystals, Dammann grating, 3D-imaging, LiDAR

**Abstract**

*We proposed a ferroelectric liquid crystal Dammann grating (FLCDG) based polarization modulated depth-mapping system. Innovatively, the proposed FLCDG enables LiDAR as a fast one-shot capturing system (>50k frames/s) and detects the translational as well as the rotational movement. Furthermore, low fabrication cost and lightweight make this device perfectly suitable modern LiDARs, particularly for short distance.*

## 1. Introduction

Light detection and ranging (LiDAR), a laser ranging technology, adopts active laser light source to achieve three-dimensional-imaging (3D-imaging). Compared with other depth-mapping techniques [1-2], LiDAR system which shows strong anti-interference ability, high ranging accuracy, small volume and light weight has high affinity to aerospace, automatic vehicles, long-distance nanometer-scale ranging and nondestructive measurement of micro-vibration target [3-5]. For now, variable ranging methods are applied, ranging from direct-pulse method (DP), amplitude-modulated continuous wave ranging method(AMCW), phase modulation method (PM), frequency-modulated continuous wave ranging method (FMCW) and polarization modulation ranging method..

Among the approaches mentioned above, polarization-modulated laser ranging technology [6] analyzes and extracts the distance information measured by optical effects, reducing the distance error introduced by the photoelectric conversion process and the circuit system. As a result, using electro-optic modulation can effectively 1) reduce the impact of noise, 2) improve the accuracy of ranging, and 3) achieve long-distance high-precision ranging. Apart from that, it shows promising ability in using the area array detector [7] to obtain the target distance in laser 3D-imaging, which is a hot topic recently. However, bottlenecks still exist [8-9], the accuracy, response time and cost performance based on these methods are limited by some factors: laser pulse width, time resolution of time-to-digital conversion chip, detector bandwidth, shot noise and time error generated by electronic circuits.

This article discloses a high-resolution and fast-response three-dimensional-imaging (3D-imaging) system for LiDAR applications [10]. A Ferroelectric liquid crystal Dammann grating (FLCDG) based polarization modulated depth-mapping system is studied. The proposed method aims to break the barriers in following aspects, i) Substitute traditional raster scanning system with one-time scanning of the whole target, ii) Speed up the scanning process by utilizing the diffractive spot array generated by DG and FLC's electro-optic effects such as fast response and the cell-superposition. iii) Produce a flexible field of view by using switchable diffraction states of FLCDG. iv) Achieve short-distance detection, and tilt surface in real-time by switchable diffractive state of FLCDG, and lastly v) Detect specific areas with high-resolution cloud points to achieve high-feasibility detection data load. Thus, this approach can be useful for a variety of applications..

## 2. Experiment

This section describes the details about system and experimental principles.

### 2.1 FLCDG based polarization modulated depth-mapping system

The schematic diagram of the FLCDG based polarization modulated depth-mapping system is shown in Fig. 1. This system includes a transmitter having a laser and one diffractive Dammann grating component, and a receiver. Specifically, in the part of transmitter, laser is utilized as the illuminator to emit a linearly polarized light beam (wavelength=532nm). The double-cell structure includes an ESHFLC modulator without DG pattern and a FLCDG, both of them are placed between the cross polarization. This combination works as a high-speed shutter and an optic splitting apparatus to form diffractive spot matrix on a target based on diffraction order of Dammann grating. As shown in Fig. 2, the Dammann grating liquid crystal cell includes two transparent substrates coated with the current conducting layer, one patterned alignment layer coated on SD1(dissolved in dimethylformamid (2 wt %)), wherein the alignment layer is patterned to satisfy the Dammann grating phase profile. Specifically, two steps of exposure, 1). exposure without DG mask to align all the molecules in same direction.2) exposure again in perpendicular polarization direction with DG mask to rewrite the alignment. Moreover, an electric suppressed helix ferroelectric liquid crystal layer sandwiched between the said two transparent substrates. In the part of receiver, the polarization state of electro-optic provides time-resolution image returned from the target. Then the CCD camera detects the light intensity of the received spots array.

According to the comparisons of traditional and FLCDG based scanning mechanism, traditional raster scanning can be divided into two categories:1) point-by-point scanning based on single point detector.2) line-by-line scanning based on array detector [3]. Contribution to the diffraction ability DG and the fast response of FLC material, one-shot capture is achieved in this paper. Apart from that, the response time is further shortening to 5μs thanks to the cell-superposition structure (highlight part in Fig 1). Specifically, applying same driving voltage on EOM 1 and FLCDG, except time shift around several μs. The polarity of EOM 1 and FLCDG are inverse. Since light can only pass through when both of them are at on state (5μs), the pulse width of output signal can be further reduced to 5μs. That is to say, the shutter time can be reduced to several micro-second

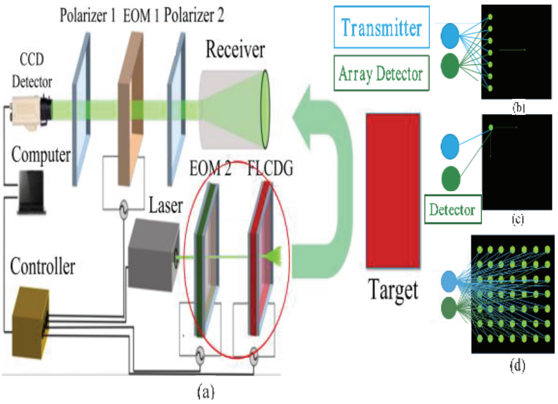


Figure 1 (a). Schematic diagram of ferroelectric Liquid crystals Dammann grating for Light Detection and Ranging Devices. (b). Traditional raster scanning: Line-by-line scanning based on an array detector. (c) Traditional raster scanning point-by-point scanning

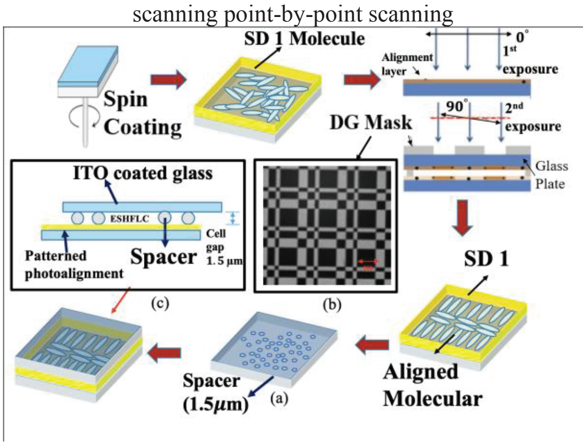


Figure 2 (a).Fabrication process of FLCDG. (b). microscopic picture of DG mask, phase difference between black and grey area is π. (c). The cell structure of the FLCDG.

### 2.2 Principle

For polarization-modulated approach, as shown in Fig. 5, when the voltage is applied across the EOM, the polarized light's phase retardation of the LC cell (EOM) is proportional to the applied voltage, which can be expressed as [5]

$$\mathrm{r} = \frac{2\pi n_0^3 r}{\lambda} V\ (t) \qquad (1)$$

In this expression, $n_0^3$ is the ordinary refractive index of the LC cell, λ is the laser light wavelength, V(t) is the voltage applied on EOM and r is electro-optic index. Since the triangular AC voltage is applied on the EOM, the relationship can be simplified as:

$$\mathrm{r} = \frac{\pi}{T_r}(t - t_0) \qquad (2)$$

(Where $T_r$ is the rise-time of applied voltage, and $t_0$ is the delay time. Since different targets with different location would have different time for round trip. Then the relationship of distance and phase retardation can be deduced based on the relationship between time and phase retardation.

$$\mathrm{r} = \frac{\pi}{D}(L - L_0) \qquad (3)$$

Where D is the initial distance induced by the gate opening. $L_0$ is the base range corresponding to the start time L is the distance between target and object.

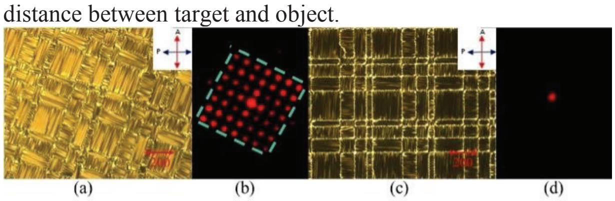


Figure 3 (a) POM (Polarizer optical diagram) of diffractive state of the FLCDG. (b) Diffraction pattern of diffractive state. (c) POM of non-diffractive state of the FLCDG. (d) Diffractive pattern of non-diffractive state.

## 3. Results

The results of the FLCDG and the verification of the method are introduced in this section. The switchable states of FLCDG are shown in Fig. 3, (a) and (b) are the micro-graph of non-diffractive state and diffractive states, respectively. Moreover, with the combination of two FLCDGs, switchable FOV and cloud points detection are achieved, the corresponding diffractive patterns are demonstrated in Fig. 4. Based on the two states and diffractive angle, setting the non-diffractive state as reference point, the relative shift of the target can be calibrated in real time according to the relative spot shift of the detected pattern. Apart from that, short-distance detection can be achieved based in this method since the spots shift is sensitive to small distance change of the target. This feature can improve the robustness in the ambient environment, close distance detection and provide fast date calibration refresh rate.

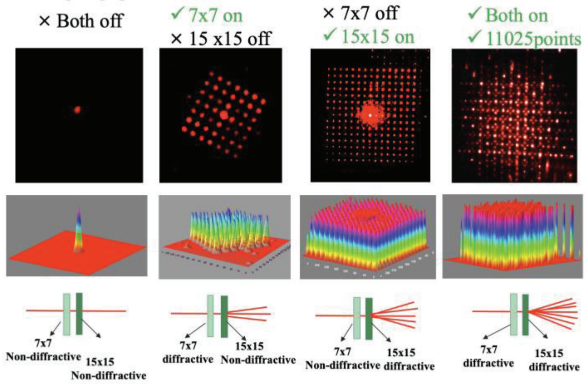


Figure 4 Diffraction pattern for combination of 7x7 and 15x15 FLCDG and corresponding intensity graph

For one spot, the relationship between intensity of polarized light and depth of the extracted information is shown in Fig. 5(a)-(b). To be specific, 10 Hz triangular wave and 500 Hz square wave are applied on EOM and FLCDG, respectively. The corresponding modulated signal with time-resolution information is received at a speed of 50µs at 5V for single FLCDG. Furthermore, this period is reduced to 5µs with combination of two FLCDG demonstrated in Fig. 5(c).After calibrating the normalized intensity map of the received real images with periodic variation. As shown in Fig. 6, the feasibility of the system is verified by comparing the intensity of polarized light and depth of the extracted information.

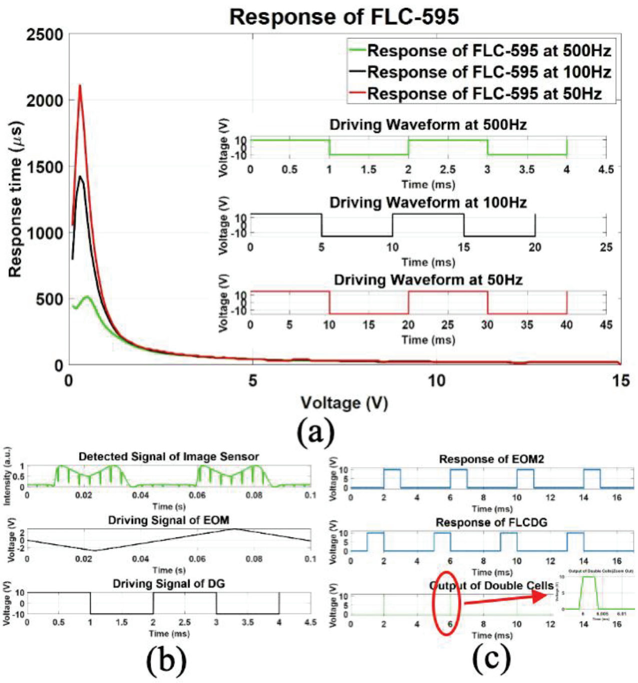


Figure 5 (a). The EO performance of ESHFLC, switching time at 5V is 50µs. (b) The EO driving scheme and EO response for the double cell FLCDG, The received signal (top), the driving electric waveform of EOM (middle) and DG (bottom) of one point. (b). The response of DG (middle) and the output of double-cell setup (bottom)

Based on the results compared with previous work, it shows promising potential for three reasons. Firstly, the scanning speed for fastest commercial LiDAR system is 2.4 million points per second [11]. The proposed method potentially has 5µs response time for 7×7 array of DG. Secondly, switchable and large front of view is achieved. Thirdly, the switchable state of FLCDG can produce switchable cloud point detection. Fourthly, real-time relative distance shift calibration is achieved due to the point shift on the diffraction pattern shown in Fig. 7. Fourthly, this point-shift feature also offers the ability to detect rotational movement shown in Fig 8. Moreover, adjusting the pitch of diffraction pattern can control the angular resolution and translational resolution here.

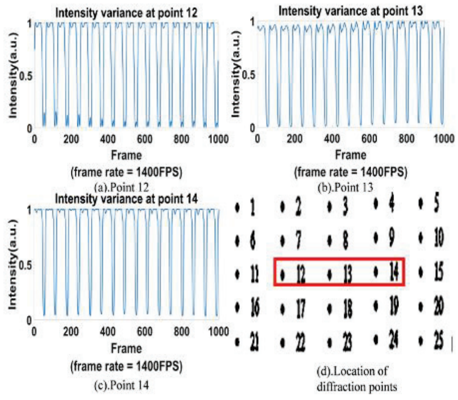


Figure 6(a)-(c). The received intensity versus shutter time of the pixels at the third row. (d) The schematic graph for corresponding sequential of the spot array generated by DG

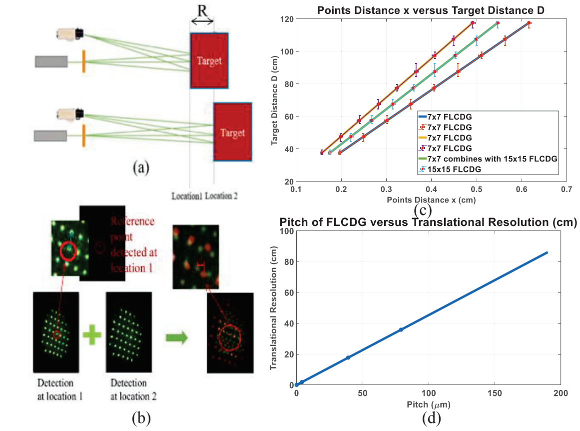


Figure 7(a). Schematic diagram of the Lidar system for detection of the translation movement of the target. (b). Detected information for real-time distance shift calibration. (c). The results of measured distance for the target (D) based on the detected spots shift (x). (d) The shows the precision in the translation motion detection of the proposed system as a function of the diffraction angle of the FLCDG

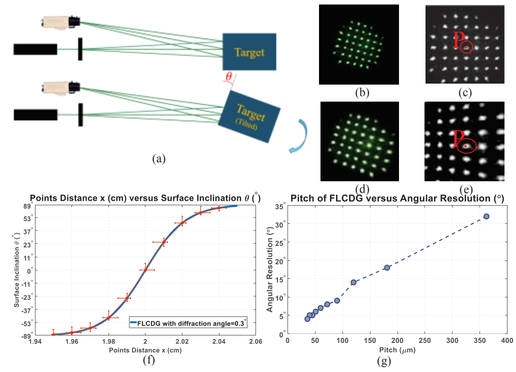


Figure 8(a) The schematic diagram for detection of the tilt of the target (Top view). (b). The captured image for the target with normal incident laser beam. (c) The calibrated image for the target without inclination angle. (d) The captured image after the the target tilting. (e) The calibrated image after the target tilting. (f) The relationship between detected pointes distance (unit: cm) and surface inclination (unit: rad). The distance from receiver to the target is 80cm. (g) shows the simulation results for the angular precision of the proposed system as a function of the diffraction angle of the grating. The red circle corresponds to the results shown in (f).

## 4. Conclusion

In this article, we disclosed a fast-switchable Lidar system based on diffraction of the FLCDG that enables us to capture the 3D information by one-shot capturing. Innovatively, a combination of FLC modulator and FLCDG high-speed shutter, makes our system seriously faster than any other alternatives. We achieved the response time of 5µs, the frame frequency can potentially reach 50k frames/s, regardless of the sampling speed of the detector. The proposed approach has three advantages over the conventional LiDAR systems. First, the fast data collection by replacing the raster scanning system with one-shot capturing the whole target. Table 1 compares the proposed FLCDG LiDAR system with other systems. The biggest advantage short distance and tilt detection. The equal intensity pattern distribution of the FLCDG results in lower diffraction point intensity that decreases with increasing diffraction points and maybe a problem for the long-range high-resolution detection. Fortunately, due to the fast-electro-optical response of the FLC, the time-sequential addressing of FLCDG can be used to solve this issue. The fast response time of FLCDG is highly suitable for the time-sequential addressing with a high frequency of 50kHz. Moreover, real-time relative distance calibration can be achieved by switching the diffraction patterns of the FLCDG. The precision of translational and angular detection depends on the pitch of FLCDG and can be seriously increased for the small pitch. In the present case, with the grating pitch of 120µm, we have been able to achieve 10 cm and 14° of translational and angular precision, respectively. The precision can be seriously improved for the smaller FLCDG pitches. Thus, the one-shot capturing system based on FLCDG is a promising candidate for LiDAR and 3D imaging applications that can find applications in a variety of devices, particularly for indoor applications such as robotics

**Table 1.** The speed comparison of commercial product and proposed method

| Method | Points /frame | Frames /s | Points /s | Precision | Range /m | Year | Ref. |
|---|---|---|---|---|---|---|---|
| Commercial (OS1-16, resolution :2048) | 27306 | 12 | 327680 | <10cm | 0.25-120 | 2020 | [3] |
| FMCW LiDAR | 252 | 714 | 180k | mm | Long range | 2017 | [6] |
| DP | 3000 | 5-10 | 15k-30k | dm | 100-1000 | 2018 | [7] |
| PM | / | 1-10 | / | cm | >0.15 | 2017 | [8] |
| Flash LiDAR | 60 | 1.5K | 90M | cm | 20-150 | 2019 | [9] |
| MEM+OPA | 1024 | 1K | 1.024 M | cm | / | 2017 | [10][11] |
| DGFLC(7x7) | 49 | 50k | 2.45M | mm | >0.12* | 2020 | This work |
| | | 10k | 500K | mm | | | |
| 15x15 | 225 | 50k | 11.2M | mm | >0.11* | 2020 | This work |
| | | 10k | 2.2M | mm | | | |
| 15x15&7x7 | 11025 | 50k | 551M | mm | >0.10* | | This work |
| | | 10k | 110M | mm | | | |
| | | 2k* | 22M | mm | | | |

* Depends on the laser spot size and diffraction angle which is controlled by pitch of FLCDG during fabrication. In the present case the laser spot laser spot size is 1mm. The diffraction angle for DGFLC 7x7, 15x15 and 15x15&7x7 are0.3°(pitch = 120µm), 0.23° (pitch = 150µm)and 0.26°, respectively.


## Acknowledgements

We acknowledge the support of The State Key Laboratory of Advanced Displays and Optoelectronics through the Innovations and Technology Commission of Hong Kong. Project number: ITC-PSKL12EG02


## References


[1] Zhan F. Huang J. & Lu S. (2019). arXiv preprint arXiv:1905.04693.

[2] Huang, J., Yuan, Z., & Zhou, X. (2019). (IJTHI), 15(3), 63-76.

[3] OS1 Mid-Range High-Resolution Imaging Lidar., Ouster, Inc., San Francisco, USA, 2020, pp. 1-3.

[4] Lum, D. J., Knarr, S. H., & Howell, J. C. (2018). Optics express, 26(12), 15420-1543.

[5] Bashkansky, M., Burris, H. R., Funk, E. E., Mahon, R., & Moore, C. I. (2004). Optics communications, 231(1-6), 93-98

[6] Tamari, S., Mory, J., & Guerrero-Meza, V. (2011). ISPRS journal of photogrammetry and remote sensing, 66(6), S85-S91

[7] Sarbolandi, H.; Plack, M.; Kolb. Sensors 2018, 18, 1679

[8] S Chen Z, Liu B, Wang S, et al. Applied optics, 2018, 57(27): 7750-7757

[9] Carrara, L., & Fiergolski, A. (2019). Appl. Sci., 9(11), 2206

[10] Hutchison, D. N., Sun, J., Doylend, J. K., Kumar, R., Heck, J., Kim, W., ... & Rong, H. (2016). Opt., 3(8), 887-890

[11] Heck, M. J. (2017). Nanophotonics, 6(1), 93